IEEE Access
Multidisciplinary ⋮ Rapid Review ⋮ Open Access Journal

Received 22 August 2023, accepted 13 September 2023, date of publication 18 September 2023,
date of current version 27 September 2023.

Digital Object Identifier 10.1109/ACCESS.2023.3316604

RESEARCH ARTICLE

Generalized Adaptive Disturbance Observer Based Global Terminal Sliding Mode Control for PMSM With Measurement Noise

BING WANG, (Member, IEEE), AND YINSHENG LI, (Student Member, IEEE)
College of Energy and Electrical Engineering, Hohai University, Nanjing 211100, China

Corresponding author: Yinsheng Li (15150693623@139.com)

This work was supported in part by the National Natural Science Foundation of China (NSFC) under Grant 51777058, and in part by the Six Talent Peaks Project in Jiangsu Province under Grant XNY-010.

ABSTRACT Improving the robustness and dynamic response of permanent magnet synchronous motor (PMSM) drive systems with measurement noise has become one of the research focuses. Aiming at this issue, a generalized adaptive disturbance observer (GADO) based global terminal sliding mode speed control (GTSMC) scheme is proposed for PMSM. Firstly, a novel terminal sliding surface ensuring that the initial system operates in sliding mode is introduced, and the GTSMC controller is thus derived. Further, a current decoupling controller based on the linear extended state observer (LESO) is designed to realize the accurate dynamic decoupling. Regarding the undesirable chattering of GTSMC, a disturbance attenuation scheme based on generalized adaptive disturbance observer (GADO) is proposed. The uncertain disturbances are estimated by the GADO, and equivalent compensation is introduced. Different from the conventional fixed-gain disturbance observer, the influence of measurement noise is considered and the generalized adaptive gain mechanism is introduced to the GADO. The gain of the GADO can be adaptively adjusted according to the operating state, in which the excellent dynamic response and low sensitivity to measurement noise are guaranteed. Finally, the proposed control scheme for PMSM are tested through simulation, and the results verify its excellent performances in terms of speed tracking, robustness against uncertainties, and sensitivity to measurement noise.

INDEX TERMS Permanent magnet synchronous motor, terminal sliding mode speed control, current decoupling, disturbance observer.

I. INTRODUCTION

PMSM has the advantages of high power density, small volume, simple structure and so on. It is widely applied in industrial processes, electric cars and robots [1]. The wide applications of PMSM in various fields also promote the demands for high performance control system of PMSM. The traditional PMSM control systems adopt the double closed-loop control mechanism constructed by the inner current loop and the outer speed loop, both the current controller and speed controller adopt the PID algorithm with simple structure [2], which has poor ability to deal with the complex and uncertain disturbances.

The associate editor coordinating the review of this manuscript and approving it for publication was Qinfen Lu.

The influence of uncertain disturbance on control performance has attracted the attention of automatic control experts. A large number of advanced control algorithms have been proposed and applied to PMSM (e.g., Fuzzy control [3], adaptive control [4], model predictive control [5] and sliding mode control [6], etc.). These algorithms improve the performances in different aspects. Among them, sliding mode control (SMC), as a variable structure control, is widely considered to effectively suppress the influence of unknowable disturbance and improve the robustness. Conventional SMC adopts appropriate switching control to force the system to a predetermined sliding surface [7]. Although the variable structure of SMC leads to the switching chattering, it also endows system with strong robustness. SMC is widely studied and applied to control PMSM because

of its strong robustness [8], [9], [10]. In [11], a novel sliding mode speed controller for PMSM is proposed. A new sliding mode surface and reaching law are designed to weaken the chattering and improve the dynamic characteristics. In [12], SMC is applied to the current control of PMSM, which effectively improves the current tracking ability. In [13], a sliding mode observer is designed to estimate the uncertain disturbance of PMSM.

The dynamic response of the system is determined by the sliding surface [14], [15]. Unfortunately, the conventional sliding mode surface can only guarantee that the system states exponentially converge to the equilibrium origin in infinite time [16]. High control precision and fast response are required for PMSM speed control. By introducing the idea of the terminal attractor into the neural network, [17] creates a terminal sliding mode surface to enable the system to converge to the equilibrium point in finite time. In [18], a novel terminal sliding mode speed controller (TSMC) is designed for PMSM to improve the dynamic response and tracking accuracy. The TSMC in [18] can force the system to reach the reference speed in finite time by adopting the non-singular terminal sliding surface.

In actual operating condition, PMSM inevitably suffers deviation of parameters and unforeseen external disturbance. As a result, the design of SMC must be conservative, requiring a significant switching gain to achieve sufficient robustness, which also results in the undesirable chattering [19]. Aiming at this issue, the combination of SMC with disturbance observer (DO) has emerged as the novel option and progressively got popular. In a general way, the disturbance observer-based SMC (DO-SMC) utilizes the disturbance observer to estimate the disturbance online and transmits the disturbance information to the SMC to realize the anti-disturbance compensation. Reference [20] introduces a nonlinear disturbance observer (NDO) based sliding mode controller for PMSM drives, in which a novel nonlinear gain matrix is created to enhance the ability to estimate disturbance. In [21], a DO-based adaptive non-singular terminal sliding mode control method is proposed, and the new reaching law is adopted to shorten setting time. However, the above two methods presume that the disturbance changes slowly over the sampling period. To make the theoretical analysis of error convergence simpler, even the derivative of the disturbance is disregarded. This is unrealistic and unreasonable in practical engineering because the derivative of disturbance is the critical factor affecting the estimation accuracy of DO. In [22], the Generalized proportional Integral observer (GPIO) based non-singular terminal sliding mode control is proposed, and the application of GPIO improves the damping capacity against disturbance significantly. It can be inspired that, the performances of DO-SMC rely on the estimation ability of the DO closely. At present, the various types of disturbance observers are developed and applied widely (e.g., the equivalent input disturbance-based estimator (EID) [23], the extended state observer (ESO) [24], [25], [26], [27], [28], and the basic nonlinear disturbance observer (BNDO) [29], etc.). Above mentioned disturbance observers have one common point: Their estimation ability is positively related to their observation gain [30]. Paradoxically, high observation gain will aggravate the noise pollution caused by measurement [31]. Therefore, the measurement noise constrains the further improvement of DO.

In this paper, a novel terminal sliding mode surface-based SMC speed controller is presented for the PMSM drive system. Different from the non-singular terminal sliding surface presented in [22], the proposed novel sliding surface enables the states of the system to locate on the sliding surface at the initial moment, and the reaching phase is eliminated. Thus, the global robustness is guaranteed. Additionally, the proposed global terminal sliding mode speed controller (GTSMC) allows manually adjusting the close-loop convergence time and enables the PMSM speed to track the reference speed in the predetermined finite time. Secondly, to deal with the coupling of electrical dynamics with mechanical dynamics in the presence of parametric uncertainties, a linear extended state observer (LESO) based current decoupling controller is created for the current loop. Furthermore, a novel generalized adaptive disturbance observer (GADO) based on generalized adaptive gain mechanism is created for the proposed GTSMC to decrease the switching gain and the sensitivity to measurement noise. It's worth noting that the proposed GADO operates on a principle different than the filter-based DO [31] sacrificing the response speed to reduce noise pollution. Instead, the proposed GADO adopts the same structure as LESO, and the gain of GADO can be adaptively adjusted in accordance with the closed-loop error. By this way, the sensitivity of GADO to measurement noise in steady-state is significantly reduced and the fast dynamic performance of GADO in transition-state is maintained at the same time. The main contributions of this paper are concluded as follows:

(1) The GTSMC is proposed for the speed regulation of PMSM, the global robustness and predefined-time stability of system are thus guaranteed.

(2) The complete current decoupling control scheme based on LESO is proposed to deal with the electrical dynamic coupling.

(3) The novel GADO is proposed to decrease the switching chattering of GTSMC, in which the generalized adaptive gain mechanism is introduced to mitigate the contradiction between noise sensitivity and dynamic performance.

The organization of this paper is as follows: In Section II, the mathematical model with parametric uncertainties of PMSM is studied. The GTSMC speed controller and LESO-based current decoupling controller are constructed in Section III. The GADO is designed for the GTSMC speed controller in Section IV. Section V verifies the effectiveness of the proposed method through simulation, and the conclusion of this paper is drawn in Section VI.

II. THE MATHEMATICAL MODEL OF PMSM WITH PARAMETRIC UNCERTAINTIES

To simplify the analysis of the mathematical model of PMSM, the following assumption is made,

Assumption 1: The impacts of magnetic saturation and flux leakage of PMSM is ignored, thus the internal magnetic field is sinusoidal.

According to the *Assumptions 1* and [1], the nominal mathematical model of PMSM in the synchronous rotation $d-q$ reference coordinate is represented as follows:

$$\begin{cases} \dot{w}_e = f_1 i_{qs} - f_2 w_e - f_3 T_L \\ \dot{i}_{qs} = -f_4 i_{qs} - f_5 w_e + f_6 v_{qs} - w_e i_{ds} \\ \dot{i}_{ds} = -f_4 i_{ds} + f_6 v_{ds} + w_e i_{qs} \end{cases} \tag{1}$$

where, $f_1 = 3p^2\varphi_f/8J, f_2 = B/J, f_3 = p/2J, f_4 = R_s/L_s, f_5 = \varphi_f/L_s, f_6 = 1/L_s$.The mechanical and electrical parameters of the PMSM nominal system are listed as follows: R_s is the stator resistance, L_s is the stator inductance, φ_f is the permanent magnet flux, i_{ds} and i_{qs} are the $d-q$ axial components of the stator current, J is the moment of inertia, B is the damping coefficient, w_e is the electrical angular velocity, T_L is the load torque, p is the number of poles.

Considering that the parametric uncertainties and modeling errors of PMSM exist, the mathematical model of PMSM can be introduced as follows:

$$\begin{cases} \dot{w}_e = f_1 i_{qs} - f_2 w_e - f_3 T_L + \delta_{w_e} \\ \dot{i}_{qs} = -f_4 i_{qs} - f_5 w_e + f_6 v_{qs} - w_e i_{ds} + \delta_q \\ \dot{i}_{ds} = -f_4 i_{ds} + f_6 v_{ds} + w_e i_{qs} + \delta_d \end{cases} \tag{2}$$

where, δ_{w_e}, δ_q and δ_d are the internal disturbances caused by uncertain parameters and modeling errors, namely,

$$\begin{cases} \delta_{w_e} = \Delta f_1 i_{qs} - \Delta f_2 w_e - \Delta f_3 T_L + f_{w_e} \\ \delta_q = -\Delta f_4 i_{qs} - \Delta f_5 w_e + \Delta f_6 v_{qs} + f_q \\ \delta_d = -\Delta f_4 i_{ds} + \Delta f_6 v_{ds} + f_d \end{cases} \tag{3}$$

where, f_{w_e}, f_q and f_d are the modeling errors.

Defining the lumped disturbances of mechanical(i.e. w_e) and electrical(i.e. i_{ds} and i_{qs}) dynamics of (2) as follows:

$$\begin{cases} d_{w_e} = -f_3 T_L + \delta_{w_e} \\ d_q = \delta_q \\ d_d = \delta_d \end{cases} \tag{4}$$

Further, (2) can be rewritten as

$$\begin{cases} \dot{w}_e = f_1 i_{qs} - f_2 w_e + d_{w_e} \\ \dot{i}_{qs} = -f_4 i_{qs} - f_5 w_e + f_6 v_{qs} - w_e i_{ds} + d_q \\ \dot{i}_{ds} = -f_4 i_{ds} + f_6 v_{ds} + w_e i_{qs} + d_d \end{cases} \tag{5}$$

In actual engineering, mechanical and electrical parameters mainly change with temperature. Thus, the derivatives of δ_{w_e}, δ_q and δ_d are bounded and continuous. It is assumed that the derivative of T_L exists and is continuous. From the above, the derivatives of d_{w_e}, d_q and d_d are bounded and continuous. The following *Assumption 2* is made for designing control scheme.

Assumption 2: i_{ds} and i_{qs} can be measured without noise while w_e can be measured by sensors with certain amount of noise.

In the practical PMSM drive systems, the three-phase current can be directly measured by electric galvanometers, its time constant is small and accuracy is high. Therefore, we consider that no noise will be introduced in the current measurement process. In the speed measurement, the physical sensors are utilized to convert the angular velocity into electrical signals. This measure will inevitably introduce measurement error, that is, noise. Therefore, the *Assumption 2* is in line with the practical engineering environment.

III. DESIGN OF GTSMC SPEED CONTROLLER AND LESO BASED CURRENT DECOUPLING CONTROLLER FOR PMSM

The control scheme for PMSM in this paper adopts a double closed-loop control mechanism, in which the current loop and the speed loop are cascaded. The block diagram of the double closed-loop control mechanism is shown in Fig. 1. In which, the ASR and the ACR represent the speed controller and current controller, respectively. The GTSMC speed controller for the speed loop and the LESO-based current decoupling controller for the current loop are introduced in this section.

A. GTSMC SPEED CONTROLLER

A new type of terminal sliding surface with finite convergence time is designed for the speed controller.

The mechanical dynamic extracted from (5) is as follows:

$$\dot{w}_e = f_1 i_{qs} - f_2 w_e + d_{w_e} \tag{6}$$

Defining $x_1 = w_e$ as the state of (6) and $u_w = i_{qs}$ as the control law. Then (6) can be rewritten as

$$\dot{x}_1 = f_1 u_w - f_2 x_1 + d_{w_e} \tag{7}$$

Defining the reference speed as $x_{1d} = w_e^*$ and the tracking error as $e_w = x_1 - x_{1d}$, the mission of the GTSMC speed controller designed in this section is to enable x_1 to track x_{1d} in a finite time.

The terminal sliding surface is designed as follows,

$$\sigma(e_w, t) = e_w - p(t) \tag{8}$$

where, $p(t)$ is the designed time-varying trajectory function for e_w and satisfies the follow *Condition 1*.

Condition 1: $p(t) \in C(R_+), \dot{p}(t) \in L_\infty$. For constant T, $p(t)$is a bounded function in period of $[0, T]$. In addition, $p(t)$ *satisfies that* $p(0) = e_w(0), \dot{p}(0) = \dot{e}_w(0)$.

The time-varying trajectory function $p(t)$ satisfying *Condition 1* enables the system to locate on the sliding mode surface at the initial moment. Then, the following time-varying trajectory function $p(t)$ is constructed based on

the *Condition 1*:

$$p(t) = \begin{cases} e_w(0) + \dot{e}_w(0)t \\ +[\frac{a_{00}}{T^2}e_w(0) + \frac{a_{01}}{T}\dot{e}_w(0)]t^2 \\ +[\frac{a_{10}}{T^3}e_w(0) + \frac{a_{11}}{T^2}\dot{e}_w(0)]t^3, \quad 0 \le t \le T \\ 0, \quad t > T \end{cases} \tag{9}$$

Consider that $p(t)$ is continuous and differentiable at $t = T$, thus $a_{ij}, i, j = 0,\ 1$ can be solved according to

$$p(T) = 0, \quad \dot{p}(T) = 0 \tag{10}$$

By solving the two equations of (10), the following results are yield

$$\begin{cases} a_{00} = -3 \\ a_{10} = 2 \end{cases} \quad \begin{cases} a_{01} = -2 \\ a_{11} = 1 \end{cases}$$

Remark 1: According to the previous design process, the system is placed on the sliding mode surface at the initial moment, i.e, $\sigma(e_w, 0) = e_w(0) - p(0) = 0$. By designing the appropriate sliding mode control law, it can be ensured that $e_w = p(t), t \ge 0$. Thus T is the moment when e_w converges to zero according to (9). In other words, the e_w can be guaranteed to converge in finite time by setting T.

Selecting the following Lyapunov function for (6)

$$V = \frac{1}{2}\sigma^2 \tag{11}$$

The time derivative of V along system (6) is

$$\begin{aligned} \dot{V} &= \sigma\dot{\sigma} = \sigma[\dot{e}_w - \dot{p}(t)] \\ &= \sigma[\dot{x}_1 - \dot{x}_{1d} - \dot{p}(t)] \\ &= \sigma[f_1 u_w - f_2 x_1 + d_{we} - \dot{p}(t)] \end{aligned} \tag{12}$$

Consequently, the following GTSMC control law is created:

$$u_w = \frac{1}{f_1}[f_2 x_1 + \dot{x}_{1d} + \dot{p}(t) - (K_1 + \gamma)sign(\sigma) - K_2\sigma] \tag{13}$$

where, K_1 and K_2 are the sliding mode switching gain and the exponential approach coefficient respectively, which satisfy that $K_1 > 0, K_2 > 0$. γ is the disturbance rejection term satisfying $\gamma \ge |d_{we}|$.

From (12) and (13), the time derivative of V is

$$\begin{aligned} \dot{V} &= \sigma[d_{we} - (K_1 + \gamma)sign(\sigma) - K_2\sigma] \\ &\le -K_1|\sigma| - K_2\sigma^2 \end{aligned} \tag{14}$$

Thus, $\dot{V}$ is negative. According to the sliding mode control theory [7], the GTSMC control law enables the terminal sliding mode surface (8) to be reachable. Further, according to *Condition 1* and REMARK 1,it is easy to know that

$$\sigma(0) = e_w(0) - p(0) = 0 \tag{15}$$

Therefore, $\sigma \equiv 0, \forall t \ge 0$, that is, the closed-loop system operates in sliding mode at the initial moment, which is the most essential and outstanding advantage of the proposed GTSMC speed controller. We can derive that the tracking error e_w will always move along the predetermined path $p(t)$.

According to (9), e_w and $\dot{e}_w$ must be continuous during the operation, otherwise it will cause the system to deviate from the sliding mode surface, which will result in the loss of valuable global robustness. Although the system can return to the sliding mode under the action of u_w.

The selection of γ depends on the upper bound information of $|d_{we}|$, however it is difficult to estimate $|d_{we}|$ in practical engineering. In this case, large γ must be selected to enable sliding surface to be reachable. This way will undoubtedly increase the conservatism and cause undesirable chattering. In section IV, a generalized adaptive disturbance observer (GADO) will be introduced to collaborate with the GTSMC speed controller.

B. LESO-BASED CURRENT DECOUPLING CONTROLLER

According to (5), there exist complex coupling effects among the electrical dynamic (i.e., i_{ds} and i_{qs}) and mechanical dynamic of PMSM. These coupling effects lead to the actions of the speed controller and current controllers coupling with each other, the complexity of control is thus greatly increased. In the condition that w_e, i_{ds} and i_{qs} can be measured without noise, the conventional methods introduce feed-forward equivalent compensation to achieve dynamic decoupling. However, in practical engineering, the measurement of w_e is inevitably noisy due to the constraints of physical conditions and sensors performance. In addition, the reference model for designing the controller will deviate from the actual model due to the uncertain parameters. Because of above factors, the traditional feed-forward decoupling methods are unable to accomplish complete dynamics decoupling.

In this section, a dynamic decoupling scheme for current controllers of i_{ds} and i_{qs} based on LESO is proposed, in which the lumped disturbance different from the nominal electrical system is extended as the new state and estimated by LESO. Then the estimated lumped disturbance is directly compensated by feed-forward to achieve complete decoupling.

The dynamic equations of i_{qs} and i_{ds} extracted from (5) are as follows:

$$\dot{i}_{qs} = -f_4 i_{qs} - f_5 w_e + f_6 v_{qs} - w_e i_{ds} + d_q \tag{16}$$

$$\dot{i}_{ds} = -f_4 i_{ds} + f_6 v_{ds} + w_e i_{qs} + d_d \tag{17}$$

The current controllers are designed as

$$v_{qs} = \frac{1}{f_6}\left(f_5 w + f_4 i_{qs} + w i_{ds}\right) + u_q \tag{18}$$

$$v_{ds} = \frac{1}{f_6}\left(f_4 i_{ds} - w i_{qs}\right) + u_d \tag{19}$$

Substituting (17) and (18) into (15) and (16), respectively, we can obtain

$$\dot{i}_{qs} = f_6 u_q + d_q \tag{20}$$

$$\dot{i}_{ds} = f_6 u_d + d_d \tag{21}$$

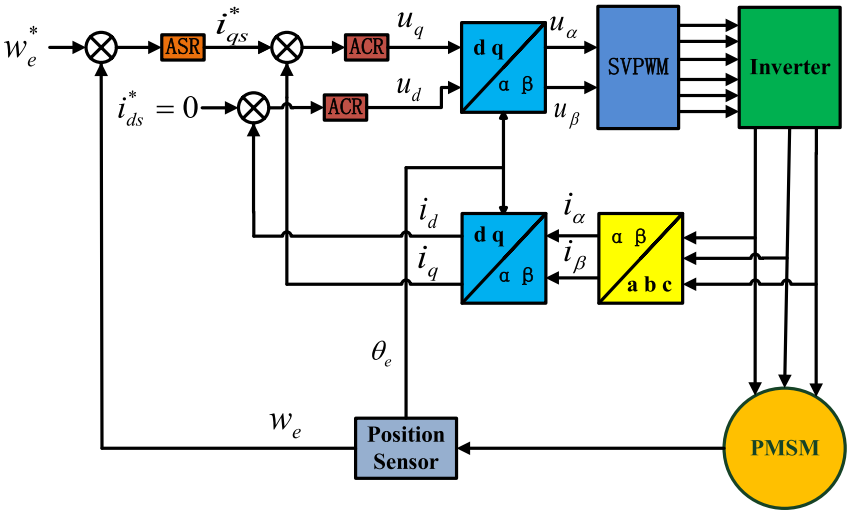

FIGURE 1. The double closed-loop control mechanism for PMSM.

In order to deal with the unknown d_d and d_q, the LESO are designed as (22) and (23) to estimate d_d and d_q respectively.

$$\begin{cases} \dot{\hat{i}}_{qs} = \hat{d}_q - 2\beta_1(\hat{i}_{qs} - i_{qs}) + f_6 u_q \\ \dot{\hat{d}}_q = -\beta_1^2(\hat{i}_{qs} - i_{qs}) \end{cases} \tag{22}$$

$$\begin{cases} \dot{\hat{i}}_{ds} = \hat{d}_d - 2\beta_2(\hat{i}_{ds} - i_{ds}) + f_6 u_d \\ \dot{\hat{d}}_q = -\beta_2^2(\hat{i}_{ds} - i_{ds}) \end{cases} \tag{23}$$

where, $\hat{i}_{qs}$, $\hat{i}_{ds}$, $\hat{d}_q$ and $\hat{d}_d$ are the estimates of i_{qs}, i_{ds}, d_d and d_q. β_1 and β_2 are the bandwidth of (22) and (23) satisfying $\beta_1, \beta_2 < 0$. It has been proved that the estimate errors $\varepsilon_1 = d_q - \hat{d}_q$ and $\varepsilon_2 = d_d - \hat{d}_d$ will asymptotically converge to zero [26].

In this paper, the current control strategy with the reference current $i_{qs}^* = u_w$ and $i_{ds}^* = 0$ is adopted. It is desirable to design the current controllers to enable i_{qs} and i_{ds} to track the reference current $i_{qs}^* = u_w$ and $i_{ds}^* = 0$.

By defining the tracking errors as $e_q = i_{qs}^* - i_{qs}$ and $e_d = i_{ds}^* - i_{ds}$, the u_q and u_d can be designed as follows based on $\hat{d}_q$ and $\hat{d}_d$:

$$u_q = -\frac{\hat{d}_q}{f_6} + k_1 e_q \tag{24}$$

$$u_d = -\frac{\hat{d}_d}{f_6} + k_2 e_d \tag{25}$$

According to [27], it is easy to prove that the tracking errors e_q and e_d will asymptotically converge to zero under the action of u_q and u_d. The block diagram of the LESO based current decoupling controller is shown in Fig. 2.

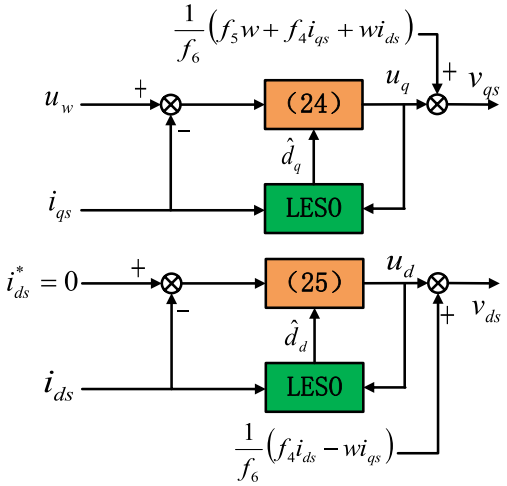

FIGURE 2. The LESO based current decoupling controller.

IV. GENERALIZED ADAPTIVE DISTURBANCE OBSERVER (GADO) FOR GTSMC SPEED CONTROLLER

The design of GTSMC speed controller depends on the upper bound information of d_{w_e} and a large switching gain is thus selected. In this section, a novel generalized adaptive disturbance observer (GADO) is designed for GTSMC speed controller to reduce the switching gain. A generalized adaptive gain mechanism is adopted in the GADO to reduce the noise sensitivity while maintaining a strong estimation capability, in light of the issue that the high gain of DO will exacerbate noise pollution.

The traditional PMSM system relies on the sensors to measure the speed in real-time. Constrained by the technical level and physical conditions, the noise will inevitably be introduced in the speed measurement process. On the other hand, general DO adopts the high-gain feedback of errors to track the disturbance rapidly. Directly introducing the output mixed with measurement noise into the high-gain feedback channel will undoubtedly worsen the noise pollution and reduce the steady-state control accuracy. Some techniques introducing filters or lowering the gain of DO can lessen

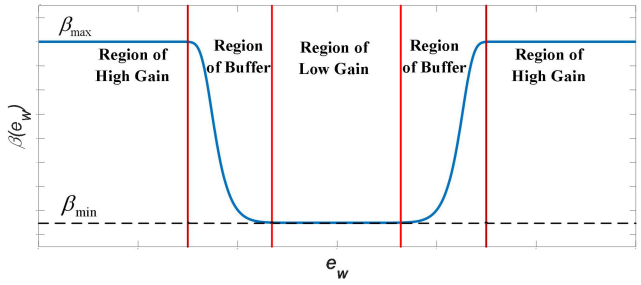

FIGURE 3. The adaptive gain $\beta(e_w)$.

noise pollution, but the dynamic response is weakened simultaneously.

A. DESIGN OF GADO

The generalized adaptive gain mechanism is presented in this paper, focusing on the problem analyzed above. In this generalized adaptive gain mechanism, the observation gain of GADO can be adjusted adaptively according to the operating state of system. That is, a large observation gain is adopted when the system is operating far from the steady-state to maintain quick dynamic response, while a small observation gain is adopted when the system is operating close to the steady-state to lessen the sensitivity to the measured noise. For PMSM, the distance of working point from the steady-state is the absolute speed-tracking error $|e_w| = |x_1 - x_{1d}|$. The generalized adaptive gain mechanism can be concluded as follows: when $|e_w|$ is small, or close to the steady-state (it should be noted that $|e_w|$ is primarily caused by the measured noise at this time), the small observation gain of GADO is adopted to reduce noise pollution; and when $|e_w|$ is large, or in the transient-state, a large observation gain is adopted to maintain the fast dynamic response.

A structure similar to LESO is adopted in the GADO. The goal of designing GADO for the GTSMC speed controller is to estimate the lumped disturbance d_{w_e} caused by modeling errors, uncertain parameters and load. According to (7), the GADO for the GTSMC speed controller can be designed as follows:

$$\begin{cases} \dot{\hat{x}}_1 = \hat{d}_{we} - 2\beta(e_w)(\hat{x}_1 - x_1) + f_1 u_w \\ \dot{\hat{d}}_{we} = -\beta^2(e_w)(\hat{x}_1 - x_1) \end{cases} \tag{26}$$

where, $\hat{d}_{we}$ and $\hat{x}_1$ are the estimation of d_{we} and x_1 respectively. $\beta(e_w)$ is the generalized adaptive gain with independent variable e_w. According to the relationship between e_w and the observation gain in the generalized adaptive gain mechanism, a novel adaptive gain is proposed as follows:

$$\beta(e_w) = p_1 + p_2\left(\frac{1}{1 + e^{-\chi|e_w|^\delta}} - 0.5\right) \tag{27}$$

where, $p_1 > 0, p_2 > 0$, χ and δ are the adjustable parameters of $\beta(e_w)$.

The adaptive gain $\beta(e_w)$ is shown in Fig. 3, which can be divided into three regions, namely, the Region of Low Gain, the Region of Buffer and the Region of High Gain. It should be noted that $\beta(e_w)$ varies gently with e_w in the Region of Low Gain, which is to reduce the sensitivity of $\beta(e_w)$ to the measured noise in steady-state. Thus, the width of the Region of Low gain should be greater than the amplitude of the measured noise. The Region of Buffer exists to distinguish the natural speed fluctuation caused by disturbance from the false speed fluctuation caused by measurement noise. Although shrinking the Region of Buffer can improve the response to disturbance, it can also easily cause confusion between the measured noise and the actual speed fluctuation brought by the disturbance. When the system enters the Region of High Gain, $\beta(e_w)$ will reach the highest value, and the estimation ability of GADO is optimal at that time.

The parameters tuning of GADO is concluded as follows: p_1 and p_2 determine the upper and lower limits of $\beta(e_w)$, that is,

$$\beta_{\min}(e_w) = p_1, \quad \beta_{\max}(e_w) = p_1 + \frac{1}{2}p_2$$

χ and δ can be utilized to adjust the width of the Region of Low Gain and Region of Buffer. We can decrease the width of the Region of Low gain and the Region of Buffer by increasing χ. And we can decrease the width of Region of Buffer and increase the width of Region of Low gain by increasing δ. In practical engineering, the width of the Region of Low Gain and the Region of Buffer should be reasonably adjusted according to the strength of measurement noise by selecting χ and δ, so as to ensure that the Region of Low Gain and the Region of Buffer can completely surround the steady-state noise. And the upper and lower limits of $\beta(e_w)$ should be determined according to the requirement on transient-state performance and steady-state noise sensitivity. We can improve the transient-state response speed and steady-state anti-noise performance by increasing $\beta_{\max}$ and decreasing $\beta_{\min}$ respectively.

B. CONVERGENCE OF ERRORS OF GADO

By defining $x_2 = d_{we}$ as the extended state, (7) can be rewritten as

$$\begin{cases} \dot{x}_1 = f_1 u_w - f_2 x_1 + x_2 \\ \dot{x}_2 = \xi \end{cases} \tag{28}$$

where, ξ is the derivative of d_{we}.

Defining the estimate errors of GADO as

$$\varepsilon = \begin{bmatrix} \varepsilon_1 \\ \varepsilon_2 \end{bmatrix} = \begin{bmatrix} \hat{x}_1 - x_1 \\ \hat{d}_{we} - x_2 \end{bmatrix} \tag{29}$$

The errors dynamic of GADO can be obtained by subtracting (30) from (26), as shown in (30)

$$\dot{\varepsilon} = A\varepsilon + D \tag{30}$$

where,

$$A = \begin{bmatrix} -2\beta(e_w) & 1 \\ -\beta^2(e_w) & 0 \end{bmatrix}, \quad D = \begin{bmatrix} 0 \\ -\xi \end{bmatrix}$$

The errors convergence of GADO is illuminated in **Theorem 1.**

Theorem 1: p_1 is selected as $p_1 > 0$, and supposing that the time derivative of d_{we} (i.e. ξ) is continuous and bounded as $\|D\| \leq \vartheta$. Then, the errors of GADO would be ultimately uniformly bounded (UUB) and forced to the following bounded neighborhood of the origin

$$B_d = \left\{ \varepsilon \in R^2 : \|\varepsilon\| \leq \frac{2\lambda_{\max}(P)}{\lambda_{\min}(P)} \vartheta \right\}$$

where, P is the positive definite matric satisfying the following equivalent Algebraic Riccati equation (ARE)

$$PA + A^T P = -Q < 0 \tag{31}$$

Proof of Theorem 1: Since $\beta_{\min}(e_w) = p_1 > 0$, the system matric A satisfies the Hurwitze condition. Thus, there must be positive definite matrices P for A to satisfy the ARE (31). Defining the following Lyapunov candidate for (30)

$$V_1 = \varepsilon^T P \varepsilon \tag{32}$$

The time derivative of V_1 is

$$\begin{aligned} \dot{V}_1 &= \dot{\varepsilon}^T P \varepsilon + \varepsilon^T P \dot{\varepsilon} \\ &= (A\varepsilon + D)^T P \varepsilon + \varepsilon^T P (A\varepsilon + D) \\ &= \varepsilon^T (A^T P + PA)\varepsilon + 2\varepsilon^T PD \\ &= -\varepsilon^T Q \varepsilon + 2\varepsilon^T PD \\ &\leq -\lambda_{\min}(Q) \|\varepsilon\|^2 + 2\lambda_{\max}(P)\vartheta \|\varepsilon\| \end{aligned} \tag{33}$$

When $\|\varepsilon\| \geq \frac{2\lambda_{\max}(P)}{\lambda_{\min}(P)}\vartheta$, $\dot{V}_1 \leq 0$.Thus, there must be $t_0 > 0$, which can lead to

$$\|\varepsilon\| \leq \frac{2\lambda_{\max}(P)}{\lambda_{\min}(P)}\vartheta, \quad \forall t \geq t_0 \tag{34}$$

Equ. (34) derives the UUB stability of estimated errors and the invariant set $B_d = \left\{ \varepsilon \in R^2 : \|\varepsilon\| \leq \frac{2\lambda_{\max}(P)}{\lambda_{\min}(P)}\vartheta \right\}$. □

Remark 2: If $\xi = 0$, the estimated errors of GADO would asymptotically uniformly converge to origin, that is

$$\lim_{t\to\infty} \|\varepsilon(t)\| = 0 \tag{35}$$

Remark 3: The UUB stability is consistent with practical engineering. It is impossible to eliminate the estimated errors completely. The ultimate estimated errors depends on the accuracy of the measuring and testing instrument.

To reduce the requirement for switching gain, the control law of (13) is modified by the lumped disturbance estimation $\hat{d}_{we}$, and the following GADO-based GTSMC control law is obtained

$$\begin{aligned} u_w = \frac{1}{f_1}[&f_2 x_1 + \dot{x}_{1d} + \dot{p}(t) - \hat{d}_{we} \\ &- (K_1 + \gamma) sign(\sigma) - K_2 \sigma] \end{aligned} \tag{36}$$

Theorem 2: By selecting $\gamma \geq \frac{2\lambda_{\max}(P)}{\lambda_{\min}(P)}\vartheta$, the GADO-based GTSMC control law (36) can ensure that the sliding surface (8) is reachable.

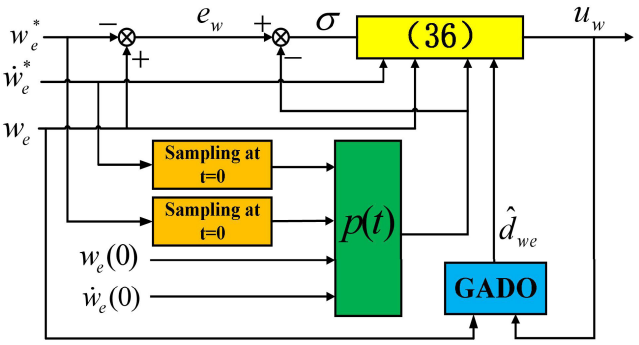

FIGURE 4. The proposed GADO-based GTSMC speed controller.

Proof of Theorem 2: According to the proof process of Theorem 1, we have the following conclusion

$$\left| d_{we} - \hat{d}_{we} \right| \leq \|\varepsilon\| \leq \frac{2\lambda_{\max}(P)}{\lambda_{\min}(P)}\vartheta, \quad \forall t \geq t_0 \tag{37}$$

And then, the time derivative of V in (11) is

$$\dot{V} = \sigma[d_{we} - \hat{d}_{we} - (K_1 + \gamma) sign(\sigma) - K_2\sigma] \tag{38}$$

Clearly, $\dot{V}$ is negative when

$$\gamma \geq \frac{2\lambda_{\max}(P)}{\lambda_{\min}(P)} \geq \left| d_{we} - \hat{d}_{we} \right|$$

Thus, according to Equ. (37), we have the conclusion that there must be $t_1 > 0$, which can lead to

$$\dot{V} \leq 0, \quad \forall t \geq t_1$$

That is, the sliding surface (8) is reachable. □

From the above analysis, the requirement for switching gain is reduced from $\gamma \geq |d_{we}|$ to $\gamma \geq \left| d_{we} - \hat{d}_{we} \right|$. In this way, the chattering issue on the sliding surface is significantly eased.

Fig. 4 depicts the block diagram of the proposed GADO-based GTSMC speed controller. The actual speed and desired speed of the PMSM are sampled at the initial moment, and the time-varying trajectory function $p(t)$ is constructed according to (9). The real-time speed and control signals are delivered to GADO for estimating the lumped disturbance $\hat{d}_{we}$. Then, combining the estimated lumped disturbance $\hat{d}_{we}$ and time-varying trajectory function $p(t)$ yields the final GTSMC control law (36).

V. SIMULATION VERIFICATION

In this section, the performances of the proposed GADO-based GTSMC scheme for PMSM in terms of speed tracking, robustness against parametric uncertainties and load, and the steady-state control accuracy influenced by measured noise is tested by simulation in MATLAB/Simulink. The parameters of PMSM for simulation are listed in Table 1. Considering that the strength of measured noise of the mainstream speed sensors in practical engineering generally does not exceed 2 rpm (the electric angular velocity is about 0.84), the adaptive gain law of GADO, as shown

TABLE 1. PMSM parameters for simulation.

Parameters	Value
Rated speed	2300
Rated load	25
R_S / Ω	0.0918
L_S / H	0.00975
$\varphi_f / V \cdot s$	0.1688
$J / kg \cdot m^2$	0.003945
$B / Ns \cdot m^{-1}$	0.0004924
p	4

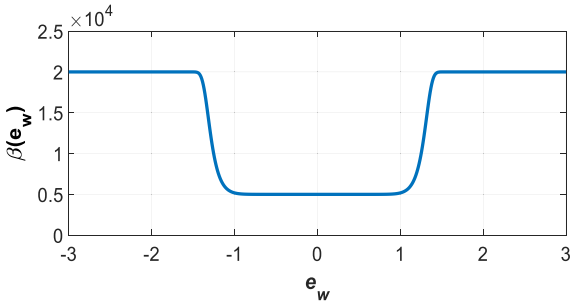

FIGURE 5. The adaptive gain law of GADO for simulation.

TABLE 2. Parameters of the GADO-based GTSMC speed controller.

Parameters of u_w	Value
K_1	20
K_2	680
γ	20
p_1	5000
p_2	30000
χ	3.5
δ	15
T	0.002s

in Fig. 5, is designed for simulation. In which, $p_1 = 5000, p_2 = 30000, \chi = 3.5$ and $\delta = 15$. The parameters of GADO-based GTSMC speed controller and LESO-based current decoupling controllers are listed in Table 2 and Table 3 respectively.

A. SPEED TRACKING PERFORMANCE

The proposed GTSMC control scheme does not allow the reference speed with step signal. To verify the speed tracking performance, the reference speed is designed to accelerate uniformly from 0rpm to 1000rpm in 0.02s. The motor starts under no-load condition. The speed responses are shown in Fig. 6, in which the proposed GADO-based GTSMC

TABLE 3. Parameters of LESO-based current decoupling controllers.

Parameters of u_q	Value	Parameters of u_d	Value
k_1	97.5	k_2	97.5
β_1	5000	β_2	5000

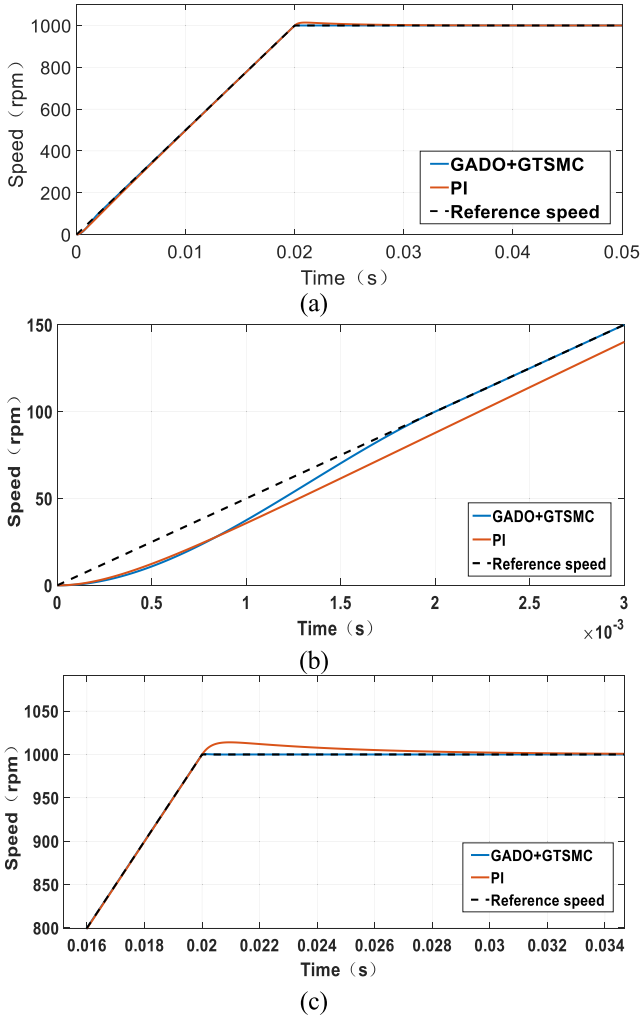

FIGURE 6. The speed response curves of GADO-based GTSMC (GADO+GTSMC) and PI: (a) Global; (b) Local amplification of the curve; (c) Local amplification of the curve.

(GADO+GTSMC) scheme is compared with the traditional PI control scheme. The comparison of speed tracking errors is shown in Fig. 7, and the curve ofσ is shown in Fig. 8.

It can be seen from Fig. 6 and Fig. 7 that the proposed GADO-based GTSMC scheme tracks the reference speed without error when $t = T = 0.002s$, which is preprogrammed. While the traditional PI scheme always has a certain amount of tracking error during the acceleration process, and the 14rpm speed overshoot occurs. The above results show the excellent tracking ability of the proposed

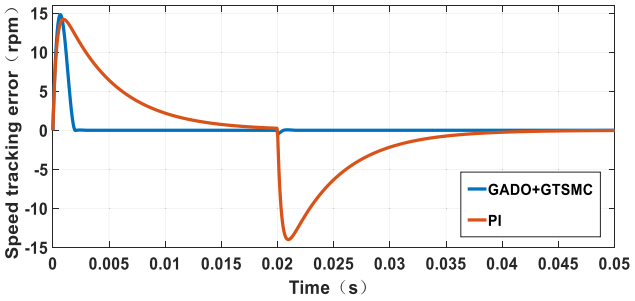

FIGURE 7. The speed tracking errors of GADO based GTSMC (GADO+GTSMC) and PI.

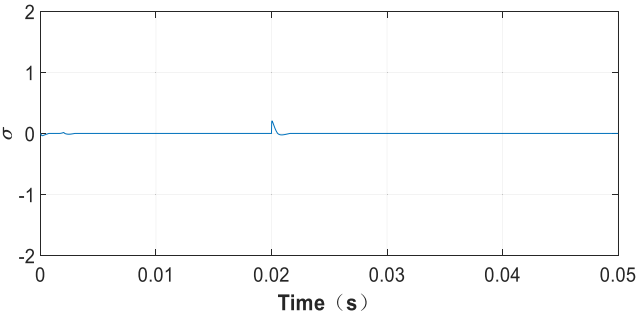

FIGURE 8. The curve of σ.

GADO-based GTSMC scheme. It can be seen from Fig. 8 that the switching function σ is located on the sliding mode surface from the initial moment. Thus it has global robustness, which is the most essential characteristic of GTSMC.

B. ROBUSTNESS AGAINST PARAMETERS

Due to the influences of temperature, mechanical friction and other factors, the internal parameters, such as the inductance L_s and permanent magnetic flux φ_f, would inevitably deviate from the nominal value to some extent during the operation. To verify the robustness against deviated parameters, the L_s and φ_f are regarded as the variable parameters. The comparative simulations of proposed GADO-based GTSMC (GADO+GTSMC) scheme, GTSMC without DO and the GTSMC based on LESO (LESO+GTSMC) with fixed gain of $\beta = 10000$ are conducted. The following operating conditions are investigated: the PMSM starts with $T_L = 10$Nm and operates stably at 1000rpm. At 0.04s, L_s mutates to 0.3 times the nominal value and φ_f mutates to 1.5 times the nominal value. At 0.07 s, L_s and φ_f recover to the nominal value. Fig. 9 shows the comparative simulation results of the proposed GADO+GTSMC scheme, GTSMC without DO (GTSMC) and LESO+GTSMC, which include the speed response curves and the lumped disturbance estimations $\hat{d}_{we}$, $\hat{d}_q$ and $\hat{d}_d$.

It can be seen from Fig. 9(a) that the proposed GADO-based GTSMC scheme shows the minimum speed fluctuation (−5.3rpm and +6rpm) and the minimum settle time (0.0035s and 0.0036s), compared with GTSMC

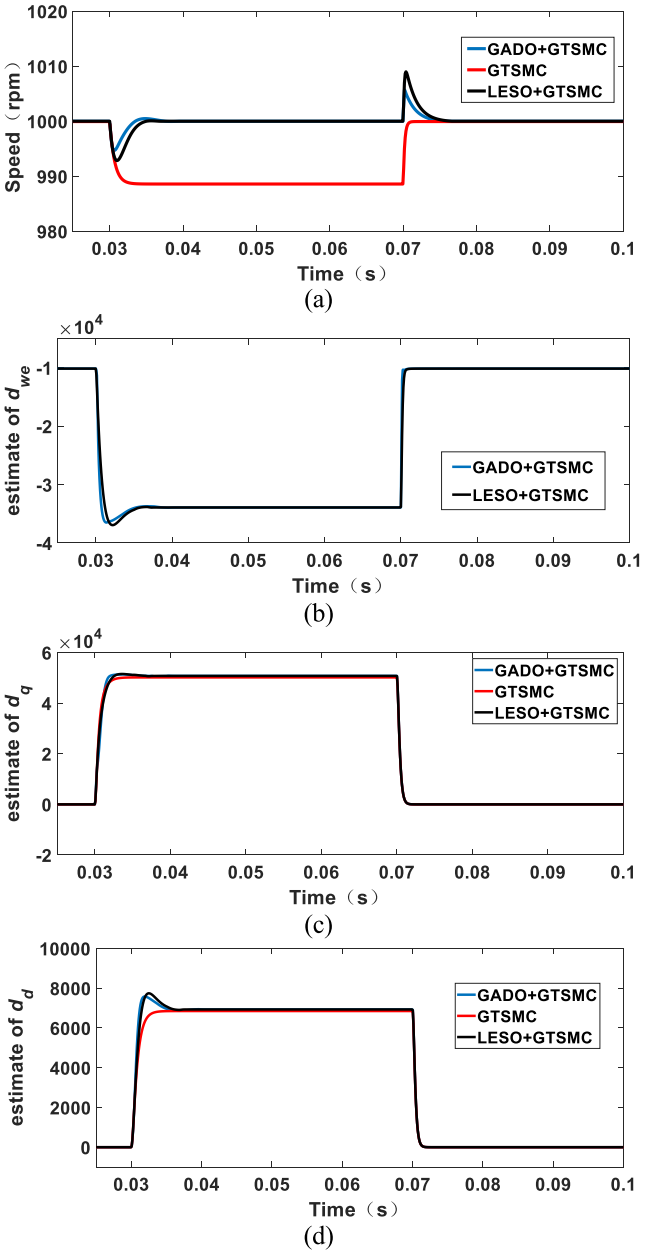

FIGURE 9. The comparative simulation results of GADO+GTSMC, GTSMC and LESO+GTSMC: (a) The speed response curves; (b) The $\hat{d}_{we}$; (c) The $\hat{d}_q$; (d) The $\hat{d}_d$.

without DO scheme (speed fluctuation is −11.4rpm and the speed cannot recover automatically) and LESO-based GTSMC scheme (the speed fluctuations are −7.1rpm and +9rpm, settle times are 0.005s and 0.0046s). The proposed GADO-based GTSMC scheme has excellent robustness against parametric perturbations. It can be seen from Fig. 9(b), (c) and (d) that the disturbance observers of both the speed controller and the current controllers can effectively estimate the uncertain disturbance caused by deviated parameters. The complete decoupling is realized.

To further reflect the robust advantages of GADO over traditional fixed gain DO, multiple groups of comparison simulations of GADO+GTSMC and LESO+GTSMC are

TABLE 4. The *ISE* of GADO+GTSMC and LESO+GTSMC.

Deviation of φ_f	*ISE* of GADO+GTSMC	*ISE* of LESO+GTSMC
$-0.9\varphi_f$	0.4044	1.274
$-0.8\varphi_f$	0.0893	0.2496
$-0.7\varphi_f$	0.0350	0.0836
$-0.6\varphi_f$	0.0188	0.0341
$-0.5\varphi_f$	0.0128	0.0148
$+2\varphi_f$	0.0019	0.0060
$+3\varphi_f$	0.0019	0.0074

implemented for different deviations of φ_f in this paper. The integral of the square speed error e_n (*ISE*) shown in (39) is used to evaluate the robustness against deviated φ_f. The *ISE* of GADO+GTSMC and LESO+GTSMC is shown in Table 4. The results demonstrate that the ability of GADO+GTSMC to cope with parametric perturbations is better than that of LESO+GTSMC.

$$ISE = \int e_n^2 d\tau \tag{39}$$

C. PERFORMANCE TO COPE WITH LOAD DISTURBANCE AND MEASUREMENT NOISE

To test the performance to cope with load disturbance and measurement noise of the proposed GADO-based GTSMC scheme, the following operating conditions are investigated: A Gaussian white noise with a variance of 0.05 and sampling time of 5E-5s is introduced to simulate the measurement noise in practical engineering; PMSM operates at 1000rpm with $T_L = 0$; The T_L steps to 25Nm at 0.4s and then declines to 5Nm at 0.5s. The comparative simulation results of proposed GADO-based GTSMC and LESO-based GTSMC are shown in Fig. 10, which include the speed response curves, the lumped disturbance estimations $\hat{d}_{we}$, control signal u_w, the current i_q and the gain of disturbance observer.

As seen in Fig. 10(a), when a sudden change in load occurs, the proposed GADO+GTSMC scheme experiences less speed fluctuation and requires less settle time than LESO+GTSMC. Thus the robustness against uncertain load of GADO+GTSMC is better than that of LESO+GTSMC. On the other hand, it is evident from Fig. 10(b), (c), and (d) that the degree of noise pollution of GADO+GTSMC is lower than that of LESO+GTSMC.

Benefiting by the generalized adaptive gain mechanism of "adopting high gain in the transition-state, adopting low gain in steady-state," which is illustrated in Fig. 10(e), GADO significantly reduces the noise pollution while maintaining its own dynamic performance.

To intuitively reflect the improvement of GADO to the steady-state control accuracy in the presence of measurement noise, the integral of square steady-state speed error (*ISSE*) shown in (40) is introduced to evaluate the steady-state

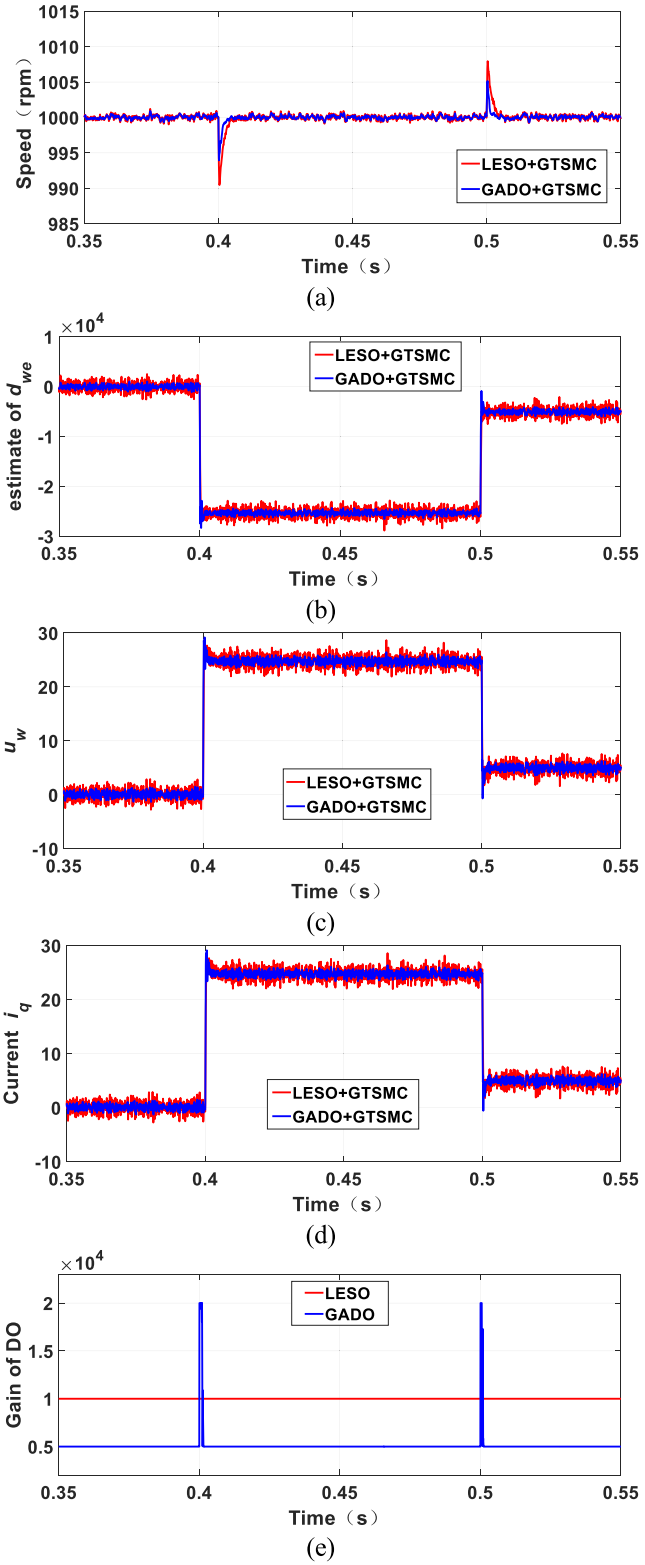

FIGURE 10. The comparative simulation results of GADO+GTSMC and LESO+GTSMC: (a) The speed response curves; (b) The $\hat{d}_{we}$; (c) The u_w; (d) The i_q; (e) The gain of disturbance observer.

control accuracy. t_0 is the time when the system reaches steady-state and it is set as $t_0 = 0.1$ for the follow simulations. The operating conditions are investigated: PMSM operates

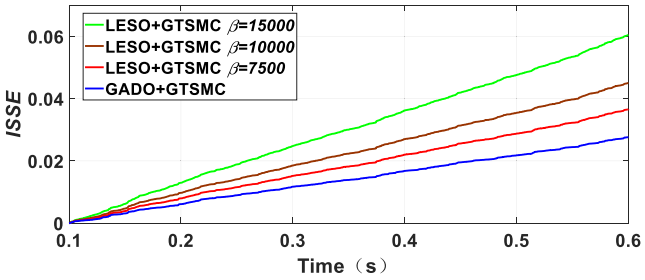

FIGURE 11. The ISSE of GADO+GTSMC and LESO+GTSMC with fixed gain of β = 7500, 10000, 15000**.**

at 1000rpm with $T_L = 0$ and a Gaussian white noise with a variance of 0.05 and sampling time of 5E-5s is introduced. The *ISSE*of the proposed GADO+GTSMC and LESO+GTSMC with fixed gain of $\beta = 5000, 10000, 15000$ are compared in Fig. 11. According to Fig. 11, the higher the gain of the DO is, the more seriously the measurement noise affects the steady-state control accuracy. Benefiting by the adaptive gain mechanism of GADO, in which the observation gain can be adjusted adaptively according to the operating state, the steady-state control accuracy of the GADO+GTSMC reaches a high level in the presence of measurement noise.

$$ISSE = \int_{t_0}^{t} e_n^2 d\tau \tag{40}$$

From the simulation results, the presented GADO based GTSMC scheme demonstrates the following advantages:

(1) The GADO based GTSMC scheme guarantees that the speed of PMSM accurately tracks the desired value at a predetermined time.

(2) The GADO based GTSMC scheme has better robustness against disturbance than the LESO based GTSMC scheme.

(3) The GADO based GTSMC scheme shows the better dynamic response against load perturbation than the LESO based GTSMC scheme.

(4) The introduction of generalized adaptive gain mechanism enables the GADO to have lower sensitivity to measurement noise than the LESO.

VI. CONCLUSION

In this paper, a global terminal sliding mode control scheme (GTSMC) for the speed control of PMSM is proposed, which ensures that the system operates on the sliding surface at initial moment. Secondly, to realize the complete dynamic decoupling control under mismatched parameters, the current decoupling controller based on LESO is designed. Further, a novel generalized adaptive disturbance observer (GADO) is proposed to reduce the requirement for switching gain. The proposed GADO can adjust the observation gain adaptively according to the operating state, which improves the dynamic performance and steady-state accuracy in the presence of measurement noise. The UUB stability of GADO and the reachability of the GTSMC scheme are proved. Finally, the proposed method is tested by simulation. The results show that the proposed GADO-based GTSMC scheme for PMSM has excellent speed tracking ability and strong robustness against the uncertain internal parameters and external load. The application of GADO effectively reduces the impact of noise pollution on steady-state control accuracy compared with traditional LESO-based control.

The proposed method has not yet been tested on the experimental platform due to the high requirements for the experimental device. In addition, the proposed GADO has limited robustness against the measurement noise with high intensity and low frequency. Future research will be devoted to verify the proposed method on the experimental platform and further improve the robustness of GADO against more severe measurement noise.

REFERENCES

[1] G. Hong, T. Wei, and X. Ding, "Multi-objective optimal design of permanent magnet synchronous motor for high efficiency and high dynamic performance," *IEEE Access*, vol. 6, pp. 23568–23581, 2018, doi: 10.1109/ACCESS.2018.2828802.

[2] E.-K. Kim, J. Kim, H. T. Nguyen, H. H. Choi, and J.-W. Jung, "Compensation of parameter uncertainty using an adaptive sliding mode control strategy for an interior permanent magnet synchronous motor drive," *IEEE Access*, vol. 7, pp. 11913–11923, 2019, doi: 10.1109/ACCESS.2019.2892749.

[3] L. Sheng, G. Xiaojie, and Z. Lanyong, "Robust adaptive backstepping sliding mode control for six-phase permanent magnet synchronous motor using recurrent wavelet fuzzy neural network," *IEEE Access*, vol. 5, pp. 14502–14515, 2017, doi: 10.1109/ACCESS.2017.2721459.

[4] S.-K. Kim, K.-G. Lee, and K.-B. Lee, "Singularity-free adaptive speed tracking control for uncertain permanent magnet synchronous motor," *IEEE Trans. Power Electron.*, vol. 31, no. 2, pp. 1692–1701, Feb. 2016, doi: 10.1109/TPEL.2015.2422790.

[5] T. Li, R. Ma, and W. Han, "Virtual-vector-based model predictive current control of five-phase PMSM with stator current and concentrated disturbance observer," *IEEE Access*, vol. 8, pp. 212635–212646, 2020, doi: 10.1109/ACCESS.2020.3040558.

[6] O. Camacho and C. A. Smith, "Sliding mode control: An approach to regulate nonlinear chemical processes," *ISA Trans.*, vol. 39, no. 2, pp. 205–218, Apr. 2000.

[7] V. Utkin, "Variable structure systems with sliding modes," *IEEE Trans. Autom. Control*, vol. AC-22, no. 2, pp. 212–222, Apr. 1977, doi: 10.1109/TAC.1977.1101446.

[8] Y. Wang, Y. Feng, X. Zhang, and J. Liang, "A new reaching law for antidisturbance sliding-mode control of PMSM speed regulation system," *IEEE Trans. Power Electron.*, vol. 35, no. 4, pp. 4117–4126, Apr. 2020, doi: 10.1109/TPEL.2019.2933613.

[9] J. Yim, S. You, Y. Lee, and W. Kim, "Chattering attenuation disturbance observer for sliding mode control: Application to permanent magnet synchronous motors," *IEEE Trans. Ind. Electron.*, vol. 70, no. 5, pp. 5161–5170, May 2023, doi: 10.1109/TIE.2022.3189074.

[10] L. Zhang, Z. Chen, X. Yu, J. Yang, and S. Li, "Sliding-mode-based robust output regulation and its application in PMSM servo systems," *IEEE Trans. Ind. Electron.*, vol. 70, no. 2, pp. 1852–1860, Feb. 2023, doi: 10.1109/TIE.2022.3163536.

[11] L. Feng, M. Deng, S. Xu, and D. Huang, "Speed regulation for PMSM drives based on a novel sliding mode controller," *IEEE Access*, vol. 8, pp. 63577–63584, 2020, doi: 10.1109/ACCESS.2020.2983898.

[12] S.-H. Chang, P.-Y. Chen, Y.-H. Ting, and S.-W. Hung, "Robust current control-based sliding mode control with simple uncertainties estimation in permanent magnet synchronous motor drive systems," *IET Electr. Power Appl.*, vol. 4, no. 6, pp. 441–450, Jul. 2010, doi: 10.1049/iet-epa.2009.0146.

[13] X. Liu, C. Zhang, K. Li, and Q. Zhang, "Robust current control-based generalized predictive control with sliding mode disturbance compensation for PMSM drives," *ISA Trans.*, vol. 71, pp. 542–552, Nov. 2017, doi: 10.1016/j.isatra.2017.08.015.

[14] J. Song, Y.-K. Wang, Y. Niu, H.-K. Lam, S. He, and H. Liu, "Periodic event-triggered terminal sliding mode speed control for networked PMSM system: A GA-optimized extended state observer approach," *IEEE/ASME Trans. Mechatronics*, vol. 27, no. 5, pp. 4153–4164, Oct. 2022, doi: 10.1109/TMECH.2022.3148541.
[15] B. Tang, W. Lu, B. Yan, K. Lu, J. Feng, and L. Guo, "A novel position speed integrated sliding mode variable structure controller for position control of PMSM," *IEEE Trans. Ind. Electron.*, vol. 69, no. 12, pp. 12621–12631, Dec. 2022, doi: 10.1109/TIE.2021.3137587.
[16] H. Hou, X. Yu, L. Xu, K. Rsetam, and Z. Cao, "Finite-time continuous terminal sliding mode control of servo motor systems," *IEEE Trans. Ind. Electron.*, vol. 67, no. 7, pp. 5647–5656, Jul. 2020, doi: 10.1109/TIE.2019.2931517.
[17] M. Zak, "Terminal attractors in neural networks," *Neural Netw.*, vol. 2, no. 4, pp. 259–274, Jan. 1989.
[18] S. Li, M. Zhou, and X. Yu, "Design and implementation of terminal sliding mode control method for PMSM speed regulation system," *IEEE Trans. Ind. Informat.*, vol. 9, no. 4, pp. 1879–1891, Nov. 2013, doi: 10.1109/TII.2012.2226896.
[19] F. Ding, J. Huang, Y. Wang, J. Zhang, and S. He, "Sliding mode control with an extended disturbance observer for a class of underactuated system in cascaded form," *Nonlinear Dyn.*, vol. 90, no. 4, pp. 2571–2582, Dec. 2017.
[20] A. T. Nguyen, B. A. Basit, H. H. Choi, and J.-W. Jung, "Disturbance attenuation for surface-mounted PMSM drives using nonlinear disturbance observer-based sliding mode control," *IEEE Access*, vol. 8, pp. 86345–86356, 2020, doi: 10.1109/ACCESS.2020.2992635.
[21] B. Xu, X. Shen, W. Ji, G. Shi, J. Xu, and S. Ding, "Adaptive nonsingular terminal sliding model control for permanent magnet synchronous motor based on disturbance observer," *IEEE Access*, vol. 6, pp. 48913–48920, 2018, doi: 10.1109/ACCESS.2018.2867463.
[22] J. Wang, L. Zhao, and L. Yu, "Adaptive terminal sliding mode control for magnetic levitation systems with enhanced disturbance compensation," *IEEE Trans. Ind. Electron.*, vol. 68, no. 1, pp. 756–766, Jan. 2021, doi: 10.1109/TIE.2020.2975487.
[23] J.-H. She, M. Fang, Y. Ohyama, H. Hashimoto, and M. Wu, "Improving disturbance-rejection performance based on an equivalent-input-disturbance approach," *IEEE Trans. Ind. Electron.*, vol. 55, no. 1, pp. 380–389, Jan. 2008.
[24] Q. Wu, L. Yu, Y.-W. Wang, and W.-A. Zhang, "LESO-based position synchronization control for networked multi-axis servo systems with time-varying delay," *IEEE/CAA J. Autom. Sinica*, vol. 7, no. 4, pp. 1116–1123, Jul. 2020, doi: 10.1109/JAS.2020.1003264.
[25] L. Qu, W. Qiao, and L. Qu, "An enhanced linear active disturbance rejection rotor position sensorless control for permanent magnet synchronous motors," *IEEE Trans. Power Electron.*, vol. 35, no. 6, pp. 6175–6184, Jun. 2020, doi: 10.1109/TPEL.2019.2953162.
[26] Z. Kuang, B. Du, S. Cui, and C. C. Chan, "Speed control of load torque feedforward compensation based on linear active disturbance rejection for five-phase PMSM," *IEEE Access*, vol. 7, pp. 159787–159796, 2019, doi: 10.1109/ACCESS.2019.2950368.
[27] J. Han, "Extended state observer for a class of uncertain plants," *Control Decis.*, vol. 10, no. 1, pp. 85–88, 1995.
[28] Z. Gao, Y. Huang, and J. Han, "An alternative paradigm for control system design," in *Proc. 40th IEEE Conf. Decis. Control*, vol. 5, Dec. 2001, pp. 4578–4585, doi: 10.1109/CDC.2001.980926.
[29] X. Chen, S. Komada, and T. Fukuda, "Design of a nonlinear disturbance observer," *IEEE Trans. Ind. Electron.*, vol. 47, no. 2, pp. 429–437, Apr. 2000, doi: 10.1109/41.836359.
[30] S. Battilotti, "Robust observer design under measurement noise with gain adaptation and saturated estimates," *Automatica*, vol. 81, pp. 75–86, Jul. 2017, doi: 10.1016/j.automatica.2017.02.008.
[31] Y. Gao, W. Wu, and Z. Wang, "Cascaded linear active disturbance rejection control for uncertain systems with input constraints and output noise," *Acta Automatica Sinica*, pp. 1–9, Aug. 2020, doi: 10.16383/j.aas.c190305.

BING WANG (Member, IEEE) was born in Yangzhou, China, in 1975. He received the B.S. degree from the Department of Automatic Control, Huazhong University of Science and Technology, in 1998, and the Ph.D. degree from the Department of Automation, University of Science and Technology of China, in 2006. Since 2006, he has been a Professor with Hohai University. His current research interests include nonlinear control, multiagent systems, and new energy technology.

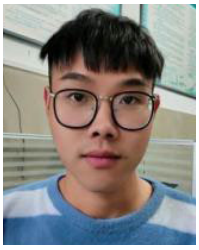

YINSHENG LI (Student Member, IEEE) was born in Jiangmen, China, in 1995. He received the B.S. degree from the College of Information Engineering, Wuyi University, in 2018, and the M.S. degree from the College of Electronic Information, Yangtze University, in 2021. He is currently pursuing the Ph.D. degree with the College of Energy and Electrical Engineering, Hohai University. His current research interests include power electronics and power transmission, active disturbance rejection control, and nonlinear robust control.